Low-temperature oxidation of [4Fe4S] analogs. Generation of a iron/sulfur cluster spectroscopically similar to the 3Fe centers in the 3Fe ferredoxins

ARTICLE *in* INORGANIC CHEMISTRY · JANUARY 1987

Impact Factor: 4.76 · DOI: 10.1021/ic00249a022

magnetic susceptibilities indicative of spin states significantly higher than $^1/_2$[19] (Table III). The room temperature magnetic susceptibility and the chemical shifts of the protons of the $(4Fe\text{-}4Se)^+$ clusters of reduced Se-substituted Cp Fd are larger than those of native reduced Cp Fd (Figure 2, Table III). These observations may be correlated with the occurrence of high-multiplicity spin states at low temperature.

At cryogenic temperatures, the reduced Se-substituted clostridial ferredoxins display three spin states, namely $S = {}^1/_2$, $S = {}^3/_2$ and $S = {}^7/_2$[3,5], and one may wonder whether a similar spin-state heterogeneity occurs at functionally relevant temperatures. The ^{1}H NMR spectra of the reduced Fd from *Bacillus polymyxa*[14] and *Bacillus stearothermophilus*,[15] which contain a single $(4Fe\text{-}4S)^+$ cluster, display eight to ten manetically shifted proton resonances, out of the 0–10 ppm range. The spectra of the reduced clostridial ferredoxins involve ca. twice as many (17–20) shifted proton resonances as those of the ferredoxins containing a single cluster[8] (Table II). It may therefrom be inferred that the two clusters in clostridial Fd differ from each other with respect to the chemical shifts of their neighboring protons. The reduced Se-substituted Cp Fd displays no more shifted proton resonances than its native counterpart (Table II), which suggests the presence of only two different types of $(4Fe\text{-}4Se)^+$ clusters in the former protein; the occurrence of three sets of spin states would imply that ca. eight to ten proton resonances have escaped observation. This seems unlikely, since no additional proton resonances have been observed in the 170–330 ppm range. Proton resonances occurring at lower field would probably be difficult to detect, due to line broadening. They would however be associated with clusters having high magnetic susceptibility, and therefore the presence of very low field resonances would result in a bulk magnetic susceptibility value even higher than the measured one (6.4 μ_B; see Table III). The ^{1}H NMR data thus show that two different spin-state ladders occur at room temperature. The relationship between these two spin ladders and the three low-temperature spin states remains to be established. In any case, the presence, in the spectra of $2[4Fe\text{-}4Se]^+$ ferredoxins, of two sets of proton resonances differing strongly by their chemical shifts and by the temperature dependencies of these shifts indicate that the $(4Fe\text{-}4Se)^+$ clusters bound to clostridial Fd polypeptide chains possess unusual magnetic properties not only at low temperature but also at room temperature. The evidence that high-spin states of $(4Fe\text{-}4X)^+$ clusters are not simply a freezing artifact, at least in the presently investigated case, clearly point to the functional relevance of the high-spin states found in some native $(4Fe\text{-}4S)^+$ proteins.[24]

Acknowledgment. We thank F. Sarrazin for assistance in obtaining the NMR spectra, M. F. Foray and J. B. Martin for helpful discussions, and J. Boyer for secretarial assistance.

(24) Lindahl, P. A.; Day, E. P.; Kent, T. A.; Orme-Johnson, W. H.; Münck, E. *J. Biol. Chem.* **1985**, *260*, 11160.

Contribution from the Laboratory for Inorganic Chemistry and Catalysis, Eindhoven University of Technology, 5600 MB Eindhoven, The Netherlands, and Gray Freshwater Biological Institute, University of Minnesota, Navarre, Minnesota 55392

Low-Temperature Oxidation of [4Fe-4S] Analogues. Generation of an Fe/S Cluster Spectroscopically Similar to the 3-Fe Clusters in the 3-Fe Ferredoxins

J. P. Weterings,[1] T. A. Kent,[2] and R. Prins*[1]

Received March 3, 1986

The oxidation of the cubane cluster compound $[Fe_4S_4(SR)_4]^{2-}$ can be directed to yield a 3-Fe cluster (i.e. a Fe/S cluster spectroscopically similar to the 3-Fe centers in the 3-Fe ferredoxins) by the choice of DMF/water as reaction medium, $K_3[Fe(CN)_6]$ as oxidant, and a low reaction temperature. The resulting compound at 4.2 and 40 K yields Mössbauer spectra that are typical for a 3-Fe cluster. At 40 K a quadrupole splitting of 0.58 mm/s and an isomer shift of 0.31 mm/s are observed. Its X-band ESR signal at $g = 2.01$ has a width of 2.8 mT and displays the same shape as that of 3-Fe proteins, including the remarkably broad wing at the high-field side of the spectrum. The influences of the reaction medium, the reagents, and the initial concentrations are discussed.

Introduction

Since 1980 it has been well established that *Azotobacter vinelandii* Fd (ferredoxin) I *crystals* contain a 3-Fe cluster[3] with an $Fe_3S_3L_6$ ring structure[4] (where L = RS^- or RO^-; Figure 1a). A second type of 3-Fe cluster with an $Fe_3S_4L_3$ cap structure (Figure 1b) has been postulated for Aconitase on the basis of EXAFS measurements.[5] This has been supported by X-ray diffraction measurements.[6] Another type of 3-Fe cluster has recently been found in denatured Aconitase and proved to have a linear structure[7] (Figure 1c). Of these three structures the cap type seems to be the most common.[8,9] It probably also is the structure of the 3-Fe cluster in *A. vinelandii* Fd I *solutions*.[9,10] The native 3-Fe structures typically display axial $S = {}^1/_2$ ESR spectra slightly above $g = 2$ with a width of about 3 mT. When first observed, these resonances were confused with the HP (high-potential protein) signal. The linear 3-Fe cluster is readily distinguished by its $S = {}^5/_2$ ESR signal around $g = 4.3$ and $g = 9.6$. Until recently it was thought that 3-Fe clusters might only

(1) Eindhoven University of Technology.
(2) Gray Freshwater Biological Institute.
(3) Emptage, M. H.; Kent, T. A.; Huynh, B.-H.; Rawlings, J.; Orme-Johnson, W. H.; Münck, E. *J. Biol. Chem.* **1980**, *255*, 1793.
(4) Stout, C. D.; Ghosh, D.; Pattabhi, V.; Robbins, A. H. *J. Biol. Chem.* **1980**, *255*, 1797.
(5) Beinert, H.; Emptage, M. H.; Dreyer, J.-L.; Scott, R. A.; Hahn, J. E.; Hodgson, K. O.; Thomson, A. J. *Proc. Natl. Acad. Sci. U.S.A.* **1983**, *80*, 393.
(6) Robbins, A. H.; Stout, C. D. *J. Biol. Chem.* **1985**, *260*, 2328.
(7) Kennedy, M. C.; Kent, T. A.; Emptage, M.; Merkle, H.; Beinert, H.; Münck, E. *J. Biol. Chem.* **1984**, *259*, 14463.
(8) Antonio, M. R.; Averill, B. A.; Moura, I.; Moura, J. J. G.; Orme-Johnson, W. H.; Teo, B.-K.; Xavier, A. V. *J. Biol. Chem.* **1982**, *257*, 6646.
(9) Johnson, M. K.; Czernuszewicz, R. S.; Spiro, T. G.; Fee, J. A.; Sweeney, W. V. *J. Am. Chem. Soc.* **1983**, *105*, 6671.
(10) Scott, R. A.; Penner-Hahn, J. E.; Hodgson, K. O.; Beinert, H.; Stout, C. D. *Springer Proc. Phys.* **1984**, *2* (*EXAFS Near Edge Struct. 3*), 105–110.

0020-1669/87/1326-0324$01.50/0

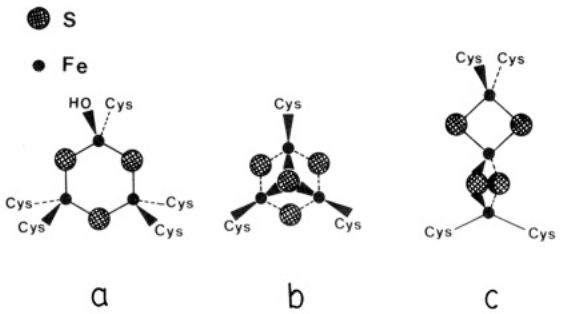

Figure 1. Structures of the ring (a), cap (b), and linear (c) 3-Fe cluster.

be degradation products, induced during protein isolation, with no biological relevance. However, in the case of succinate dehydrogenase their necessity for enzymatic activity has now been proved.[11]

Adequate model compounds for the native 3-Fe clusters have not been isolated as yet. The few compounds reported to have a cap structure[12,13] contain organic sulfur in a number of places where an analogue would have inorganic sulfur. Compounds having the ring structure either display the same property[14] or have dimerized to a prismane structure.[15] Only for the linear 3-Fe cluster has a fully satisfactory analogue been reported.[14]

Biochemically there are two reactions leading to a 3-Fe cluster. The first is self-assembly from iron, sulfide, and apoprotein.[16] We have not been able to observe this reaction with synthetic tricysteinyl peptides.[17] The second type of reaction is oxidation of cubane clusters, $[Fe_4S_4L_4]^{2-}$. Apparently the 3-Fe cluster of all known 3-Fe proteins can be formed by this reaction. Yet oxidation of cubanes does not necessarily produce a 3-Fe cluster. One-electron oxidation results in the formation of a HP^{ox} analogue if bulky ligands are employed[18] or if a special solvent prevents further reactions.[19] If halide (X^-) is provided, $[Fe_4S_4(SR)_4]^{2-}$ can be oxidized (by X_2 or another oxidant) to yield $[Fe_4S_4X_4]^{2-}$ and disulfide.[20] Further oxidation in a polar medium results in the $[Fe_2S_2X_4]^{2-}$ dinuclear species.[21] Finally, it has been reported that in nonpolar solvents cubanes can be transformed into $[Fe_6S_6L_6]^{2-}$ clusters (prismanes) before breaking up into the dinuclear species.[22] It has been pointed out that even counterions like Et_4N^+ affect the course of this reaction, probably by stabilizing intermediates instead of through selective crystallization.[23]

Clearly, the result of a cubane oxidation is strongly dependent on the exact reaction circumstances. We report here on low-temperature-oxidation reactions generating the 3-Fe cluster in solution and its characterization by ESR and Mössbauer spectroscopy.

Experimental Section

Cubane iron–sulfur clusters[24] and $[Fe(C_5H_5)_2](BF_4)$[25] were synthesized according to the literature. High-potential protein solutions of *Chromatium* strain D and *Thiocapsa roseopersicina* were kindly supplied by Dr. K. K. Rao. If not stated otherwise "buffer" signifies a 50 mM Tris·HCl solution of pH 7.5. ^{57}Fe of 95% isotopic purity was bought (as a metal) from Intersales-Holland B.V. (Hengelo, The Netherlands) and converted to $FeCl_3$ by heating (350 °C in a Cl_2 flow.[26] All other chemicals and solvents were of reagent grade, purchased from Aldrich Chemie and used without further purification.

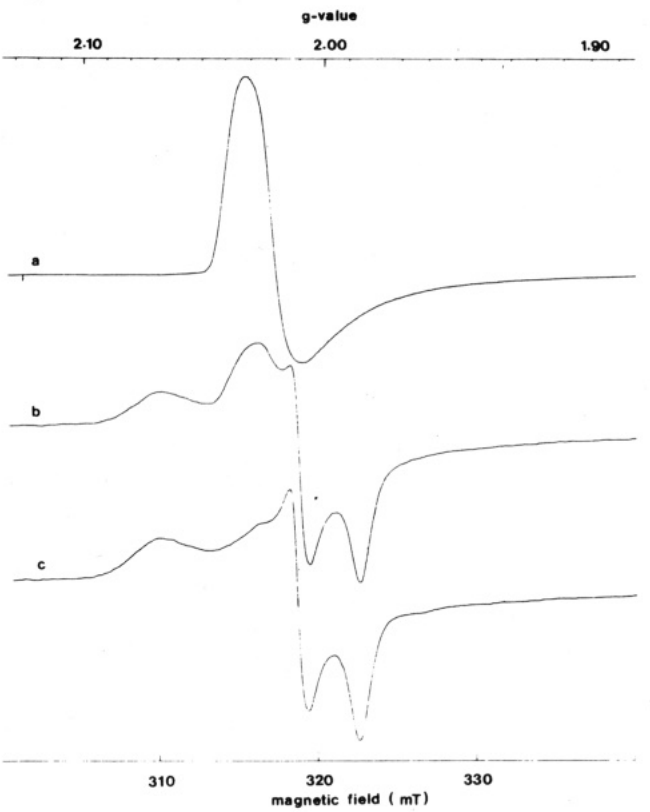

Figure 2. First-derivative ESR spectra of $[Fe_4S_4(S\text{-}t\text{-}Bu)_4]^{2-}$/DMF, 4 mM, oxidized at −40 °C by 1 equiv of $[Fe(CN)_6]^{3-}$/buffer: (a) spectrum sampled at −40 °C, gain 200; (b) spectrum after 2 min of incubation at room temperature, gain 1000; (c) spectrum after 4 min of incubation at room temperature. Spectra were measured at 4.2 K, with a microwave power of 0.5 mW.

The Mössbauer equipment has been described before.[27] Isomer shifts are quoted relative to the centroid of the spectrum of iron metal with the ^{57}Co source and the iron foil at room temperature. X-Band EPR spectra were recorded with a Varian E-15 spectrometer equipped with an Oxford Instruments ESR-9 continuous-flow cryostat. All ESR spectra were recorded at a microwave frequency of 8.970 GHz, a modulation amplitude of 0.5 mT, and a modulation frequency of 100 kHz. Copper(II) chloride was used as a quantitative reference (Merck A.A.S. standard). A BBC microcomputer was interfaced to the spectrometer for integration according to the method of moments.[28] The same computer was used for kinetical calculations.

Anaerobic handling of solutions was effected by the usual vacuum-line/syringe methods. A glass kit consisting of a sample holder and a reaction vessel connected by a siphon was immersed as a whole in an ethanol-filled Dewar. The bath was cooled by a thermostated flow of cold nitrogen gas. The standard temperature of the bath was −40 °C. Separately, nitrogen gas was flushed through a metal cooling loop (−40 °C) via the sample holder into the reaction mixture to provide mingling during the reaction. By reversal of the flow direction in the kit, a sample of the mixture could be transferred to a Mössbauer cell or to an ESR tube. The reaction in the sample was then stopped by quickly immersing it in liquid nitrogen. Once frozen, the top of the kit was opened and air was allowed in for short periods of time to enable further handling while the sample at the bottom of the kit remained at low temperature. In a typical experiment 6 mL of a 4 mM solution of $(NMe_4)_2[Fe_4S_4(S\text{-}t\text{-}Bu)_4]$

(11) Johnson, M. K.; Morningstar, J. E.; Bennett, D. E.; Ackrell, B. A. C.; Kearney, E. B. *J. Biol. Chem.* **1985**, *260*, 7368.
(12) Gerst, K.; Nordman, C. E. *Abstracts of Papers, American Crystallographic Association* Summer Meeting; American Crystallographic Association: Storrs, CT, 1974; p 225, Abstract E2.
(13) Henkel, G.; Tremel, W.; Krebs, B. *Angew. Chem., Int. Ed. Engl.* **1981**, *20*, 1033.
(14) Hagen, K. S.; Holm, R. H. *J. Am. Chem. Soc.* **1982**, *104*, 5496.
(15) Saak, W.; Henkel, G.; Pohl, S. *Angew. Chem.* **1984**, *96*, 153.
(16) Moura, J. J. G.; Moura, I.; Kent, T. A.; Lipscomb, J. D.; Huynh, B.-H.; LeGall, J.; Xavier, A. V.; Münck, E. *J. Biol. Chem.* **1982**, *257*, 6259.
(17) Weterings, J. P.; Prins, R., submitted for publication in *J. Chem. Soc., Dalton Trans.*
(18) O'Sullivan, T.; Millar, M. M. *J. Am. Chem. Soc.* **1985**, *107*, 4096.
(19) Pickett, C. J. *J. Chem. Soc., Chem. Commun.* **1985**, 323.
(20) Weterings, J. P. Ph. D. Thesis, Eindhoven University of Technology, 1986.
(21) Wong, G. B.; Bobrik, M. A.; Holm, R. H. *Inorg. Chem.* **1978**, *17*, 578.
(22) Coucouvanis, D.; Kanatzidis, M. G.; Dunham, W. R.; Hagen, W. R. *J. Am. Chem. Soc.* **1984**, *106*, 7998.
(23) Kanatzidis, M. G.; Hagen, W. R.; Dunham, W. R.; Lester, R. K.; Coucouvanis, D. *J. Am. Chem. Soc.* **1985**, *107*, 953.
(24) Christou, G.; Garner, C. D. *J. Chem. Soc., Dalton Trans.* **1979**, 1093.
(25) Hendrickson, D. N.; Sohn, Y. S.; Gray, H. B. *Inorg. Chem.* **1971**, *10*, 1559.
(26) Tarr, B. R. *Inorg. Synth.* **1950**, *3*, 191.
(27) Zimmermann, R.; Münck, E.; Brill, W. J.; Shah, V. K.; Henzl, M. T.; Rawlings, J.; Orme-Johnson, W. H. *Biochim. Biophys. Acta* **1978**, *537*, 185.
(28) Wyard, S. J. *J. Sci. Instrum.* **1965**, *42*, 769.

Table I. Spectral Components Observed[a] for the Mössbauer Sample at 40 K

spectral component	rel area, % of total ^{57}Fe	ΔE_q, mm/s	δ, mm/s	Γ(fwhm), mm/s
3-Fe	28 (3)	0.58 (2)	0.31 (2)	0.32
4-Fe	59 (3)	1.18 (2)	0.45 (2)	*b*
Fe^{2+}	13 (3)	2.4 (1)	1.2 (1)	0.6

[a] Results of a least-squares fit of symmetric Lorentzian pairs to the data of Figure 5a. If we assume the recoil-free fractions of all ^{57}Fe sites are the same, then the relative area of a given spectral component is directly proportional to the concentration of the associated ^{57}Fe. [b] The lines of the [4Fe-4S] cluster are broad and non-Lorentzian. To approximate better the line shape, we fitted these lines with two nested Lorentzian pairs of equal area. The results were $\Delta E_q(1) = 1.32$ mm/s, $\Delta E_q(2) = 1.05$ mm/s, $\delta(1) = \delta(2) = 0.45$ mm/s, and $\Gamma(1) = \Gamma(2) = 0.28$ mm/s. The average values are quoted above. An analogous fit to the 4.2 K data was done. To the first order, subtraction of the 4.2 K signal of *D. gigas* Fd II (28% total ^{57}Fe) from the spectrum of Figure 5b cancels the signal of the 3-Fe model compound. A fit to the resulting difference spectrum yielded for the [4Fe-4S] cluster $\Delta E_q(1) = 1.34$ mm/s, $\Delta E_q(2) = 1.08$ mm/s, $\delta(1) = 0.45$ mm/s, $\delta(2) = 0.46$ mm/s, and $\Gamma(1) = \Gamma(2) = 0.28$ mm/s.

in DMF (*N*,*N*-dimethylformamide) was cooled to −40 °C. One equivalent of $K_3[Fe(CN)_6]$ dissolved in 1.5 mL of buffer at room temperature was injected in one squirt to avoid freezing in the needle. Mixing water and DMF is an exothermic process. The temperature profile was meausred by a thermocouple in the reactor. It showed a jump from −40 to −22 °C upon addition of the water. After 1 min the temperature was −33 °C, and after 4 min the mixture reached −40 °C.

Results and Discussion

Stability. A sample made by the standard procedure (described under Experimental Section) and measured at 4.2 K showed the typical 3-Fe ESR spectrum depicted in the upper trace of Figure 2. A longer reaction time, up to 120 min, at −40 °C proved to be of no influence. The reaction is finished within a few minutes, and the product is stable at this temperature. Measurement at higher temperatures (>30 K) showed the presence of low concentrations of other radicals, indicating that the conversion of the cubane to the 3-Fe cluster was not complete. The fact that these species are observed at relatively high temperatures (at least up to 60 K) characterizes them as probably of organic nature. A standard sample kept at room temperature for 40 s showed a loss of two-thirds of its intensity. The elaborate sample preparation is thus justified. Incubation for 2 and 4 min at room temperature caused an almost complete disappearance of the 3-Fe signal and the dominance of the ESR spectrum by resonances from unidentified radicals (Figure 2b,c). These resonances are roughly similar to those found in excessively oxidized *A. vinelandii* Fd I.[29] They are different from reduced 2-Fe cluster signals, which usually show resonances up to *g* values of 1.89.

Variations of Reagents and Solvents. In a number of experiments the components of the standard procedure were modified one at a time. Use of $(NBu_4)_2[Fe_4S_4(SPh)_4]$ resulted in quick precipitation of a fine black powder upon the injection of the aqueous ferricyanide solution. The low-temperature ESR spectrum of this suspension showed that the oxidant was largely unreacted. After it was checked that 18-crown-6-ether is of no influence on the generation of the 3-Fe cluster, 3 equiv of it were used to keep the potassium ferricyanide in solution as the amount of water was reduced to 1%. Again the ESR spectrum showed unreacted ferricyanide. The reaction was also run at −25 °C to compensate for the absence of heat of mixture. The result was unchanged. This could be explained by the strongly diminished potential of ferricyanide in nonprotic solvents.[30] When ferricyanide was replaced by $[Fe(C_5H_5)_2](BF_4)$ or when DMF was replaced by acetonitrile, no ESR signal was observed. Reportedly, ferricyanide takes a special place among oxidants when iron–sulfur proteins are involved.[31] All deviations from our standard procedure that we tried were thus seen to be unfavorable. Isolation of the 3-Fe cluster will therefore be difficult. Furthermore, magnetic circular dichroism spectroscopy is impossible at present since DMF/water samples do not form a glass.[32]

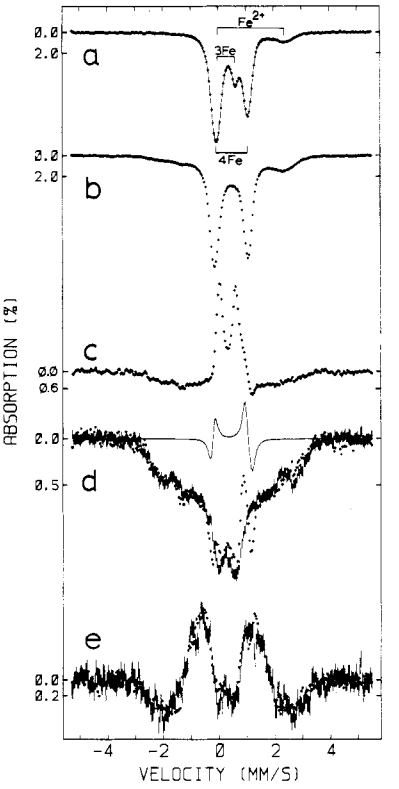

Figure 3. Mössbauer spectra of $[^{57}Fe_4S_4(S\text{-}t\text{-}Bu)_4]^{2-}$/DMF, 1 mM, oxidized at −40 °C by 1 equiv of $[Fe(CN)_6]^{3-}$/buffer. The sample was 9 mm thick when the data of spectrum e were collected. For spectra a–d, the sample was transferred while in Ar atmosphere to a cell with 2.5 times the cross sectional area. The thinner sample was needed to avoid saturation effects. The absorption scales are uncorrected for Compton background. (a) Spectrum of the sample measured at 40 K with a 60 mT magnetic field applied parallel to the γ beam. The solid line is a least-squares fit described in Table I. Three quadrupole doublets are indicated by the labeled brackets. (b) Spectrum of the same sample measured at 4.2 K with 60 mT parallel field. (c) Difference spectrum generated by substracting the 40 K data (spectrum a) from the 4.2 K data (spectrum b). The area and base line of the 40 K data were normalized to those of the 4.2 K data for the subtraction. (d) Magnetic hyperfine pattern (dots) of the synthetic 3-Fe cluster. This pattern was generated by adding a simulation of the 40 K 3-Fe signal (as described in Table I) to the spectrum c. The 4.2 K, 60 mT parallel spectrum of *D. gigas* Fd II is also plotted (hatchmarks, area normalized, data from ref 34). The sharp feature at +1 mm/s in the model compound data arises from the change of the 4-Fe cluster signal between 4.2 and 40 K. The solid line indicates the difference spectrum calculated for the 4-Fe cluster from the parameters quoted in Table I. (e) Field direction dependence of the 4.2 K spectra of the Mössbauer sample (dots). This difference spectrum was generated by subtracting the area-normalized 60 mT perpendicular applied field spectrum from the 60 mT parallel field spectrum. An analogous difference spectrum for *D. gigas* Fd II (hatchmarks) is plotted with normalized height. This Fd II spectrum and Figure 2 of ref 34 are from the same data set.

Mössbauer Spectra. A Mössbauer sample was prepared (standard procedure) from a 1 mM solution of ^{57}Fe cubane. The spectrum of this sample at 40 K is shown in Figure 3a and comprises three quadrupole doublets. The right lines of the three doublets are partially resolved while the left lines are not. The results of a least squares fit to these data are given in Table I. The largest doublet accounts for 59% ± 3% total ^{57}Fe and is characteristic of diamagnetic [4Fe-4S] clusters. The rightmost

(29) Morgan, T. V.; Stephens, P. J.; Devlin, F.; Stout, C. D.; Melis, K. A.; Burgess, B. K. *Proc. Natl. Acad. Sci. U.S.A.* **1984**, *81*, 1931.
(30) Mascharak, P. K. *Inorg. Chem.* **1986**, *25*, 245.
(31) Sweeney, W. V.; Bearden, A. J.; Rabinowitz, J. C. *Biochem. Biophys. Res. Commun.* **1974**, *59*, 188.
(32) Johnson, M. K., personal communication.

line in Figure 3a indicates that 13% ± 3% total ^{57}Fe is high-spin ferrous iron that is not associated with either 4-Fe or 3-Fe clusters. The third doublet with ΔE_q = 0.58 mm/s and δ = 0.31 mm/s is characteristic of tetrahedral sulfur-coordinated ferric iron[33] and accounts for 28% ± 3% total ^{57}Fe. As shown below this doublet is the signal of a 3-Fe cluster.

At 4.2 K (Figure 3b) the signals of the [4Fe-4S] cluster and the ferrous iron have changed little from those of the 40 K data. The [4Fe–4S] cluster line at +1 mm/s is slightly shifted (see Table I). The ferric doublet, however, has been replaced by a broad magnetic pattern. This transition from fast to slow relaxation between 40 and 4.2 K would be very unusual for monoferric iron. Figure 3c shows the difference spectrum generated by subtracting the 40 K spectrum from the 4.2 K data. In the difference spectrum, the signals of the [4Fe-4S] cluster and the ferrous iron essentially cancel and the magnetic pattern is clearly illustrated. Our best representation (Figure 3d) of the magnetic hyperfine pattern was generated by adding a theoretical simulation of the 3-Fe cluster 40 K doublet to the spectrum of Figure 3c. This pattern is very similar to those of known 3-Fe clusters.[34,35] Direct comparison with the spectrum of *Desulfovibrio gigas* Fd II shows the two spectra are virtually identical.

Further evidence for the presence of a 3-Fe cluster is provided by the field direction dependence of the 4.2 K spectra. The data of Figure 3e is the difference between a spectrum recorded with the 60 mT applied field parallel to the gamma beam and one with the field perpendicular. With constant temperature and weak applied field, the signals of both the [4Fe-4S] cluster and the Fe^{2+} cancel very well. The strong field direction dependent signal proves that the associated iron belongs to the ESR-active center.[36] Direct comparison again shows that the hyperfine interactions observed for this component of the model are, within the noise, identical with those of the *D. gigas* Fd II 3-Fe cluster.

We also recorded data at 4.2 K and 6 T applied field (data not shown). One component of the paramagnetic pattern clearly moved outward relative to the 60-mT data. This increase in splitting shows that the internal field for that comonent is positive and is proof that the corresponding iron site is part of a spin-coupled system.[36] Taken together with the ESR data, the Mössbauer spectra of Figure 3 are very strong evidence that the sample contained roughly 28% total ^{57}Fe in the form of a 3-Fe cluster with paramagnetic properties very similar to those of the *D. gigas* Fd II 3-Fe cluster.

ESR Spectra. Ferredoxins from a large number of sources have been reported to show the so-called g = 2.01 signal. Among these are *Methanosarcina barkeri*[37] (4 × 5.5 kDa), *Desulfovibrio gigas*[16,36] (4 × 6 kDa), *Clostridium pasteurianum*[38] (6 kDa), *Desulfovibrio africanus*[39] (2 × 6.75 kDa), *Thermus thermophilus*[40] (10 kDa), *Pseudomonas ovalis*[41] (12 kDa), *Mycobacterium smegmatis*[42] (12 kDa), *Mycobacterium flavum*[43] (13.5 kDa), and of course *A. vinelandii*[44] (14.5 kDa). Two forms of the g = 2.01 signal can be distinguished: an almost isotropic form having $g_\parallel < g_\perp$ and a form in which an extra shoulder can be distinguished on the $g_\parallel$ peak. The high-field part of the spectrum is often quite broad. Higher molecular weight 3-Fe proteins, for instance aconitase[45] (66–89 kDa), *Chromatium vinosum* hydrogenase[46] (62 kDa), and most probably *Vibrio succinogenes* fumarate reductase[47] (79 + 31 + 2 × 25 kDa), also display ESR signals slightly above g = 2, but their shapes are different. Figure 2a shows the spectrum of our 3-Fe preparation. It is close to those of the Fds.

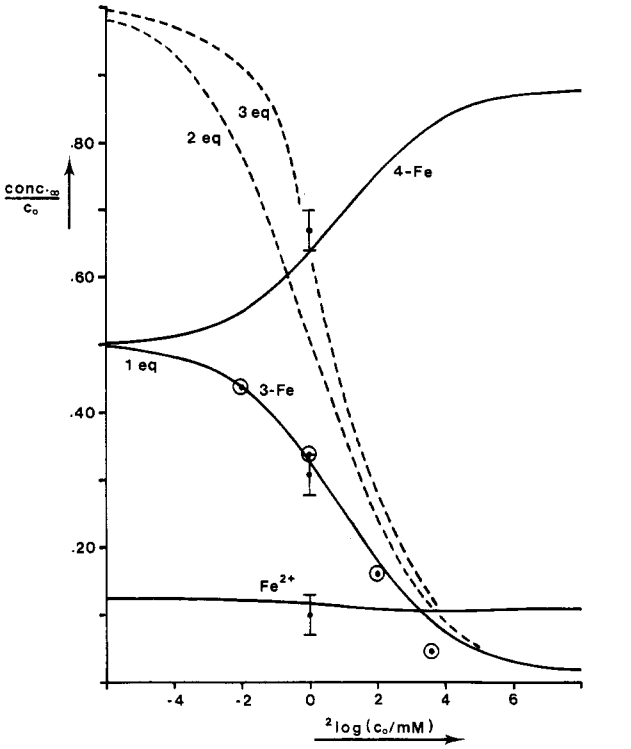

Figure 4. Product distribution at the end of the reaction of cubane and 1 equiv of oxidant as a function of initial cubane concentration c_0. Bars indicate Mössbauer data; ESR data are encircled. Solid curves are the predictions from the kinetic model described in the text. Dashed curves are predictions of the 3-Fe cluster yield if 2 and 3 equiv of ferricyanide are added to the cubane, based on the model fitting the 1-equiv curve.

The relaxation of the synthetic 3-Fe center was analyzed[20] and macroheterogeneity[48] was convincingly demonstrated. This macroheterogeneity and the flatness of the low-field top of the spectrum suggests at least two **g** tensors are required to fit the spectrum (as is the case for HP[49]). A reliable explanation of the 3-Fe ESR spectrum cannot come from computer fits only; it requires more knowledge of the electronic and structural properties of the cluster.

Three-iron Fds have been reported to show an almost isotropic spectrum or one with a shoulder. Apparently the spectrum of our model is of the isotropic type. The disappearance of the shoulder from the protein spectra could be a matter of broadening (overall or in the low-field region only). The spectra of *D. gigas* Fd II seem to be almost isotropic for the ^{57}Fe-reconstituted protein[16] whereas a shoulder can be discerned for the ^{56}Fe protein.[36]

Since the g = 2.01 signal has often been called HP-like, we examined the ESR signal of HP under a variety of circumstances. Different protein sources and different pH values caused only minor changes in the well-known spectrum. Denaturation at room

(33) Schulz, C.; Debrunner, P. G. *J. Phys., Colloq.* **1976**, *37*, C6-154.
(34) Beinert, H.; Thomson, A. J. *Arch. Biochem. Biophys.* **1983**, *222*, 333.
(35) Huynh, B.-H.; Moura, J. J. G.; Moura, I.; Kent, T. A.; LeGall, J.; Xavier, A. V.; Münck, E. *J. Biol. Chem.* **1980**, *255*, 3242.
(36) Münck, E. *Iron-sulfur Proteins*; Spiro, T. G., Ed.; Wiley-Interscience: New York, 1982; Chapter 4.
(37) Moura, I.; Moura, J. J. G.; Huynh, B.-H.; Santos, H.; LeGall, J.; Xavier, A. V. *Eur. J. Biochem.* **1982**, *126*, 95.
(38) Johnson, M. K.; Spiro, T. G.; Mortenson, L. E. *J. Biol. Chem.* **1982**, *257*, 2447.
(39) Hatchikan, E. C.; Cammack, R.; Patil, D. S.; Robinson, A. E.; Richards, A. J. M.; George, S.; Thomson, A. J. *Biochim. Biophys. Acta* **1984**, *784*, 40.
(40) Hille, R.; Yoshida, T.; Tarr, G. E.; Williams, C. H., Jr.; Ludwig, M. L.; Fee, J. A.; Kent, T. A.; Huynh, B.-H.; Münck, E. *J. Biol. Chem.* **1983**, *258*, 13008.
(41) Ohmori, D. *Biochim. Biophys. Acta* **1984**, *790*, 15.
(42) Imai, T.; Matsumoto, T.; Ohta, S.; Ohmori, D.; Suzuki, K.; Tanaka, J.; Tsukioka, M.; Tobari, J. *Biochim. Biophys. Acta* **1983**, *743*, 91.
(43) Yates, M. G.; O'Donnell, M. J.; Lowe, D. J.; Bothe, H. *Eur. J. Biochem.* **1978**, *85*, 291.
(44) Sweeney, W. V.; Rabinowitz, J. C.; Yoch, D. C. *J. Biol. Chem.* **1975**, *250*, 7842.
(45) Ruzicka, F. J.; Beinert, H. *J. Biol. Chem.* **1978**, *253*, 2514.
(46) Albracht, S. P. J. *Biochem. Soc. Trans.* **1985**, *13*, 582.
(47) Albracht, S. P. J.; Unden, G.; Kröger, A. *Biochim. Biophys. Acta* **1981**, *661*, 295.
(48) Beinert, H.; Orme-Johnson, W. H. *Magnetic Resonance in Biological Systems*; Ehrenberg, A., Malmström, B. G.; Vångård, T., Eds.; Pergamon: New York, 1967.
(49) Antanaitis, B. C.; Moss, T. H. *Biochim. Biophys. Acta* **1975**, *405*, 262.

temperature by urea also had little effect on the spectral shape though the intensity of the signal diminished. The spectrum of *Chromatium* HP denatured in dimethyl sulfoxide has been reported to be similar to the reduced 4-Fe signal.[50] Whether this spectrum is due to destruction products or to the unconstrained $[Fe_4S_4]^{3+}$ core is uncertain. However, this does not affect our conclusion: an $[Fe_4S_4]^{3+}$ cluster has, to the best of our knowledge, not yet been shown to yield an ESR spectrum similar to those of known 3-Fe clusters.

Kinetics. The product distribution determined by Mössbauer spectroscopy gives an important clue to the kinetics of 3-Fe formation. The data for a reaction starting with 1 mM cubane and 1 equiv of oxidant are shown in Table I. If a 4-Fe cluster yields one 3-Fe cluster and one Fe(II) ion, then 28% iron in 3-Fe cluster demands 9.3% Fe(II). Of the 13% Fe(II) found, a small part thus seems to originate from complete destruction of cubanes. Only complete oxidation to disulfide and sulfur, at the same time producing Fe(II), allows for the consumption of all oxidant and the observed large amounts of residual cubane. Actually, in order to balance the oxidant and 28% Fe in 3-Fe clusters, one would expect to find 12% Fe(II) and 60% Fe in 4-Fe clusters.

A second source of information on the kinetics is the dependence of 3-Fe yield on the initial concentrations of cubanes and oxidant (always 1 equiv). This was monitored by ESR. The Mössbauer and ESR data are presented in Figure 4 together with calculated curves based on the following model. Oxidation (by Ox) of cubane (Cub) first yields a HP^{ox} analogue (Hip). The observed concentration dependence is then explained by taking into consideration two consecutive reactions of different order. First, the reaction of Ox with Hip is assumed to give a labile species that immediately falls apart. Upon reduction of Fe(III) by released ligands, 8 equiv (S^{2-} and RS^-, denoted Lig) remain to be oxidized. Second, Hip itself could excrete one Fe(II) and one ligand thus yielding the trinuclear species (Tri). Finally, free ligands are oxidized.

$$\text{Cub} + \text{Ox} \rightarrow \text{Hip} \quad (1)$$

$$\text{Hip} + \text{Ox} \rightarrow 8\text{Lig} \quad (2)$$

$$\text{Hip} \rightarrow \text{Tri} + \text{Lig} \quad (3)$$

$$\text{Lig} + \text{Ox} \rightarrow \text{S, RSSR} \quad (4)$$

At high concentrations, the HP-analogue is mainly converted via the bimolecular reaction 2 and the yield of 3-Fe cluster is vanishingly low. At low concentrations, reaction 2 is of no importance and the course of reactions is essentially

$$\text{Cub} + \text{Ox} \rightarrow \text{Tri} + \text{Lig} \quad (5)$$

$$\text{Lig} + \text{Ox} \rightarrow \text{S, RSSR} \quad (6)$$

Assuming the latter reaction to be fast relative to the former it can be seen that the yield of 3-Fe cluster is limited to 50%. (Note that always 1 equiv was used.) The steepness of the curves in Figure 4 and the midpoint concentration are governed by the reaction rate constants k_i. Denoting the reaction rates by

$$A = k_1[\text{Cub}][\text{Ox}] \qquad B = k_2[\text{Hip}][\text{Ox}] \qquad C = k_3[\text{Hip}]$$
$$D = k_4[\text{Lig}][\text{Ox}]$$

the differential equations describing the kinetics take the following form

$$d[\text{Cub}]/dt = -A \qquad d[\text{Ox}]/dt = -A - B - D$$
$$d[\text{Tri}]/dt = C \qquad d[\text{Hip}]/dt = A - B - C$$
$$d[\text{Lig}]/dt = 8B + C - D$$

The course of the concentrations was computed by numerical integration. The reaction was considered to be ended when [Ox] < 0.1% and [Hip] < 0.1%, or when [Cub] < 0.1% and [Hip] < 0.1%. The ratio of k values fitting the experimental results best was: $k_1:k_2:k_3:k_4$ = 1:60:250 mM:100. The unit mM remains in the ratio because of the difference in reaction order; the unit of time is arbitrary.

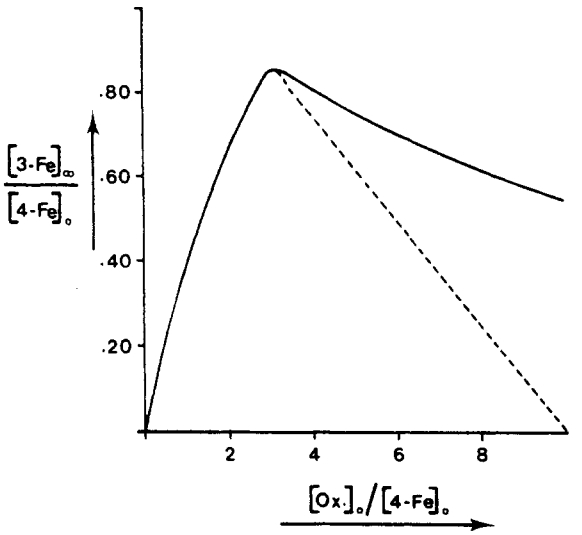

Figure 5. Prediction of the 3-Fe cluster yield as a function of the number of equivalents of oxidant at 0.5 mM initial concentration of cubane: solid curve, calculated from the four-reaction model; dashed line, corrected for the slow oxidation of 3-Fe cluster.

According to our model, addition of several equivalents of oxidant improves the 3-Fe yield. Curves for 1, 2, and 3 equiv are shown in Figure 4. The improvement depends on the concentration of cubane, reaching almost complete conversion at extremely low concentrations and being unchanged in the high-concentration limit. Figure 5 shows the 3-Fe yield as a function of the number of equivalents of oxidant at a constant initial cubane concentration of 0.5 mM. At low numbers of equivalents, the oxidant is completely consumed and cubane is left over. At the top of the curve, at about $3^1/_4$ equiv both are consumed. At high equivalent numbers, oxidant is left over. Since it is to be expected that this amount of redundant oxidant will attack 3-Fe cluster in the long run, the model was extended with the reaction

$$\text{Tri} + \text{Ox} \rightarrow 7\text{Lig} \quad (7)$$

This reaction must be very slow with respect to the sequence (1)–(4). Therefore the effect of (7) was included by subtracting one-eighth of the amount of redundant oxidant from the 3-Fe yield (dashed curve).

Recognizing the fact that reaction 3 is the only one leading to a 3-Fe cluster, we tried to separately carry out this reaction. HP was oxidized with somewhat less than 1 equiv of ferricyanide. The solution was then injection in DMF at −40 °C, and the ice formed dissolved at the lowest temperature possible. Neither a HP^{ox} nor a 3-Fe cluster ESR signal was found. When the protein was first denatured in cold DMF and then oxidized the result was the same. Since both 4-Fe and 3-Fe clusters are now known to be stable under these circumstances, we conclude that the impetuous unfolding of the protein causes the rupture of clusters. Dissolving the HP-analogue[18] in DMF/water (4:1) at −40 °C could be a more successful approach if the bulky ligands do not prevent the separation of just one iron–ligand pair.

Conclusions

Oxidation of $[Fe_4S_4(S\text{-}t\text{-}Bu)_4]^{2-}$ by $[Fe(CN)_6]^{3-}$ in DMF/buffer (4:1) at −40 °C yields a new cluster that is spectroscopically similar to the [3Fe-*x*S] cluster. This 3-Fe complex is stable at −40 °C and unstable at room temperature. It could not be obtained in a different medium or by using other oxidants. An attempt to prepare it by denaturation of oxidized HP also failed. This preparation is the first and (as yet) only one yielding a manageable and relatively highly concentrated solution of a synthetic 3-Fe cluster.

Both ESR and Mössbauer spectroscopic data of the model compound are consistent with assignment to a 3-Fe structure. Moreover the kinetics demand an intermediate $[Fe_4S_4]^{3+}$ cluster,

(50) Cammack, R. *Biochem. Soc. Trans.* **1975**, *3*, 482.

thereby ruling out the possibility of a HP analogue being the endproduct. Furthermore, HP under several denaturing circumstances did not show an ESR spectrum similar to those of 3-Fe proteins. This strongly indicates that the new compound described in this work is indeed a 3-Fe cluster. It also implies that ESR spectra of iron–sulfur clusters are not easily changed by the surroundings as is often assumed. We therefore believe that the first ESR spectrum reported for a synthetic 3-Fe cluster was the one published by Cammack et al.,[51] whereas the spectra shown by Christou et al.[52] most probably were neither those of a HP nor those of a 3-Fe cluster.

The kinetics justify the expectation that even higher conversions of 4-Fe to 3-Fe could be attained. Alternatively the 3-Fe cluster might be produced from a HP analogue in a controlled-degradation reaction. Isolation and elucidation of the structure then come within reach.

Acknowledgment. We gratefully acknowledge the cooperation of Drs. K. K. Rao and M. K. Johnson and thank Drs. P. H. M. Budzelaar and E. Münck for helpful discussions. This study was supported by the Netherlands Foundation for Chemical Research (SON) with financial aid from the Netherlands Organization for the Advancement of Pure Research (ZWO) and by National Science Foundation Grant No. NSF/DMB8306964.

Registry No. $(NMe_4)_2[Fe_4S_4(S\text{-}t\text{-}Bu)_4]$, 52678-92-9; $K_3[Fe(CN)_6]$, 13746-66-2; $(NBu_4)_2[Fe_4S_4(SPh)_4]$, 52586-83-1.

(51) Cammack, R.; Christou, G. *Hydrogenases: Their Catalytic Activity, Structure, and Function*; Schlegel, H. G., Schneider, K., Eds.; Erich Goltze: Göttingen, BRD, 1978; pp 45–56.
(52) Christou, G.; Garner, C. D.; Drew, M. G. B.; Cammack, R. *J. Chem. Soc., Dalton Trans.* **1981**, 1550.

Notes

Contribution from the Department of Chemistry, Manipur University, Imphal 795 003, India

Studies on the Alkylation of Vitamin B_{12s} and Related Systems Revisited: Novel Features of Oxidative-Addition Reactions

Dipankar Datta* and G. Tomba Sharma†

Received June 26, 1986

Vitamin B_{12} is a Co(III) complex of the corrin moiety. It is the only vitamin known to contain a metal center. Its chemistry[1,2] is so fascinating and challenging that there seems to be unabated constant interest in this vitamin and its derivatives to workers of various disciplines of chemistry since its isolation in 1948 (for a comprehensive study, see ref 1; a few selected aspects are covered in ref 2). This vitamin can exist in three different oxidation states—the Co(I) variety is known as B_{12s}. Alkylation of vitamin B_{12s} (schematically represented by reaction 1) gives rise to a

$$(Co^{I})^{-} + RX \longrightarrow \underset{\mathbf{1}}{\overset{R}{|}(Co)} + X^{-} \qquad (1)$$

Co(III) species with a metal–carbon bond through an oxidative reaction mechanism.[3a] It may be mentioned in this connection that coenzyme B_{12}, which has such a metal–carbon bond, and methylcobalamin (R = CH_3 in **1** of eq 1), which is a substrate in the methionine biosynthesis are nature's only organometallic compounds known to date.[3a]

Extensive studies carried out by Schrauzer and co-workers[4] led to the earlier conclusion that reaction 1, which is reversible,[5] proceeds through an S_N2 mechanism (eq 2). Later observation

$$(Co^{I}) + RX \longrightarrow \left[X \cdots R \cdots Co \right]^{*} \longrightarrow \overset{R}{|}(Co) + X^{-} \qquad (2)$$

of inversion of configuration at the reacting carbon center by Jensen et al.[6] supported this view. However, they seemed to have missed the electron-transfer component of such reactions, and "attempts to demonstrate the expected inversion of configuraion at carbon resulting from these oxidative additions led to"[7] such erroneous conclusions.[7–9] Herein we reanalyze the data of Schrauzer and co-workers[4] to obtain certain interesting features of the alkylation reaction and the oxidative additions, in general.

Table I. Variation of the Rate Constants of the Alkylation of Tributylphosphine–Cobaloxime$_s$ with Alkyl Halides (RX)[a]

R group	σ^{*} [b]	log k		
		Cl	Br	I
$-CH_3$ (**1**)	0.000	−0.070	2.340	3.360
$-C_2H_5$ (**2**)	−0.100	−2.046	0.204	
$-CH_2CH_2CH_3$ (**3**)	−0.115	−2.201	0.174	
$-CH(CH_3)_2$ (**4**)	−0.190	−3.495	−0.959	0.505
$-CH_2CH_2CH_2CH_3$ (**5**)	−0.130	−2.137		
$-CH(CH_3)CH_2CH_3$ (**6**)	−0.210			−0.086
$-CH_2CH(CH_3)_2$ (**7**)	−0.125	−3.110	−0.553	0.924
$-CH(CH_3)CH{=}CH_2$ (**8**)		0.778		
$-CH_2C_6H_5$ (**9**)	0.215	2.640	4.280	
$-CH(CH_3)C_6H_5$ (**10**)	0.110	0.360		
$-CH(C_6H_5)_2$ (**11**)	0.405	0.000		
$-CH_2CN$ (**12**)	1.300	3.204		
$-CH_2CONH_2$ (**13**)	0.600	1.146		

[a] Meanings of the symbols used are same as in the text. Rate data are taken from ref 4. [b] In case of $-CH_2CONH_2$ σ^{*} has been calculated from the σ_I data (0.27) given in Table 16 of: Charton, M. *Prog. Phys. Org. Chem.* **1981**, *13*, 119. The formula $\sigma_I(X) = 0.45\sigma^{*}$ ($-CH_2X$) of Taft (Taft, R. W.; Lewis, I. C. *J. Am. Chem. Soc.* **1958**, *80*, 2436) was used. Others are taken from ref 13.

† An FIP fellow.

(1) Dolphin, D., Ed. *B_{12}*; Wiley-Interscience: New York, 1982; Vol. 1 and 2.
(2) Stevens, R. V.; Chang, J. H.; Lapalme, R.; Schow, S.; Schlageter, M. G.; Shapiro, R.; Weller, H. N. *J. Am. Chem. Soc.* **1983**, *105*, 7719. Scheffold, R.; Orlinski, R. *J. Am. Chem. Soc.* **1983**, *105*, 7200. Jorim, E.; Schweiger, A.; Gunthard, Hs. H. *J. Am. Chem. Soc.* **1983**, *105*, 4277. Balasubramanian, P. S.; Gould, E. S. *Inorg. Chem.* **1984**, *23*, 824. Halpern, J.; Kim, S. H.; Leung, T. W. *J. Am. Chem. Soc.* **1984**, *106*, 8317. Parker, W. O., Jr.; Bresciani-Pahor, N.; Zangrando, E.; Randacio, L.; Marzilli, L. G. *Inorg. Chem.* **1985**, *24*, 3908. Christianson, D. W.; Lipscomb, W. N. *J. Am. Chem. Soc.* **1985**, *107*, 2682. Halpern, J. *Science* (Washington, D.C.) **1985**, *227*, 869. Baldwin, D. A.; Betterton, E. A.; Chemaly, S. M.; Pratt, J. M. *J. Chem. Soc., Dalton Trans.* **1985**, 1613.
(3) (a) Huheey, J. E. *Inorganic Chemistry: Principles of Structure and Reactivity*, 3rd ed.; Harper and Row: New York, 1983; pp 878–880. (b) *Ibid.* pp 137–160.
(4) Schrauzer, G. N.; Deutsch, E.; Windgassen, R. J. *J. Am. Chem. Soc.* **1968**, *90*, 2441. Schrauzer, G. N.; Deutsch, E. *J. Am. Chem. Soc.* **1969**, *91*, 3341.
(5) Stadlbauer, E. A.; Holland, R. J.; Lamm, F. P.; Schrauzer, G. N. *Bioinorg. Chem.* **1974**, *4*, 67.
(6) Jensen, F. R.; Madan, V.; Buchanan, D. H. *J. Am. Chem. Soc.* **1970**, *92*, 1414.

0020-1669/87/1326-0329$01.50/0